EUROPEAN ORGANIZATION FOR NUCLEAR RESEARCH

CERN-PPE/97-08
20 January 1997

The Spin-Dependent Structure Function $g_1(x)$ of the Deuteron from Polarized Deep-Inelastic Muon Scattering

The Spin Muon Collaboration (SMC)

Abstract

We present a new measurement of the spin-dependent structure function g_1^{d} of the deuteron from deep inelastic scattering of 190 GeV polarized muons on polarized deuterons. The results are combined with our previous measurements of g_1^{d}. A perturbative QCD evolution in next-to-leading order is used to compute $g_1^{\mathrm{d}}(x)$ at a constant Q^2. At $Q^2 = 10\,\mathrm{GeV}^2$, we obtain a first moment $\Gamma_1^{\mathrm{d}} = \int_0^1 g_1^{\mathrm{d}} \mathrm{d}x = 0.041 \pm 0.008$, a flavour-singlet axial charge of the nucleon $a_0 = 0.30 \pm 0.08$, and an axial charge of the strange quark $a_{\mathrm{s}} = -0.09 \pm 0.03$. Using our earlier determination of Γ_1^{p}, we obtain $\Gamma_1^{\mathrm{p}} - \Gamma_1^{\mathrm{n}} = 0.183 \pm 0.035$ at $Q^2 = 10\,\mathrm{GeV}^2$. This result is in agreement with the Bjorken sum rule which predicts $\Gamma_1^{\mathrm{p}} - \Gamma_1^{\mathrm{n}} = 0.186 \pm 0.002$ at the same Q^2.

Submitted to Physics Letters B

The Spin Muon Collaboration (SMC)

D. Adams[19], B. Adeva[21], T. Akdogan[2], E. Arik[2], A. Arvidson[24,a], B. Badelek[24,26], M.K. Ballintijn[16], D. Bardin[9,b], G. Bardin[20,†], G. Baum[1], P. Berglund[7], L. Betev[12], I.G. Bird[20,c], R. Birsa[23], P. Björkholm[24,d], B.E. Bonner[19], N. de Botton[20], M. Boutemeur[28,e], F. Bradamante[4,23], A. Bravar[10], A. Bressan[23,f], S. Bültmann[1,g], E. Burtin[20], C. Cavata[20], D. Crabb[25], J. Cranshaw[19,h], T. Çuhadar[2], S. Dalla Torre[23], R. van Dantzig[16], B. Derro[3], A. Deshpande[28], S. Dhawan[28], C. Dulya[3,16], A. Dyring[24], S. Eichblatt[19,i], J.C. Faivre[20], D. Fasching[18,j], F. Feinstein[20], C. Fernandez[21,8], B. Frois[4,20], A. Gallas[21], J.A. Garzon[21,8], T. Gaussiran[19], M. Giorgi[23], E. von Goeler[17], F. Gomez[21], G. Gracia[21], N. de Groot[16,k], M. Grosse-Perdekamp[3,l], D. von Harrach[10], T. Hasegawa[13,m], P. Hautle[4,n], N. Hayashi[13,o], C.A. Heusch[4,p], N. Horikawa[13], V.W. Hughes[28], G. Igo[3], S. Ishimoto[13,q], T. Iwata[14], E.M. Kabuß[10], T. Kageya[13], L. Kalinovskaya[r], A. Karev[9], H.J. Kessler[5], T.J. Ketel[16], J. Kiryluk[26], A. Kishi[14], Yu. Kisselev[9], L. Klostermann[16,s], D. Krämer[1], V. Krivokhijine[9], W. Kröger[4,p], V. Kukhtin[9], K. Kurek[26], J. Kyynäräinen[4,7,t], M. Lamanna[23], U. Landgraf[5], J.M. Le Goff[4,20], F. Lehar[20], A. de Lesquen[20], J. Lichtenstadt[4,22], T. Lindqvist[24], M. Litmaath[16,u], M. Lowe[19,j], A. Magnon[20], G.K. Mallot[10], F. Marie[20], A. Martin[23], J. Martino[20], T. Matsuda[13,m], B. Mayes[8], J.S. McCarthy[25], K. Medved[9], G. van Middelkoop[16], D. Miller[18], K. Mori[15], J. Moromisato[17], A. Nagaitsev[9], J. Nassalski[26], L. Naumann[4,†], T.O. Niinikoski[4], J.E.J. Oberski[16], A. Ogawa[14], C. Ozben[2], D.P. Parks[8], F. Perrot-Kunne[20], D. Peshekhonov[9], R. Piegaia[28,v], L. Pinsky[8], S. Platchkov[20], M. Plo[21], J. Polec[26], D. Pose[9], H. Postma[16], J. Pretz[10], R. Puntaferro[23], T. Pussieux[20], J. Pyrlik[8], G. Rädel[4], A. Rijllart[4], J.B. Roberts[19], S. Rock[4,w], M. Rodriguez[24,x], E. Rondio[4,26], A. Rosado[12], I. Sabo[22], J. Saborido[21], A. Sandacz[26], I. Savin[9], P. Schiavon[23], K.P. Schüler[28,y], R. Seitz[10,z], Y. Semertzidis[4,A], F. Sever[16,B], P. Shanahan[18,i], E. P. Sichtermann[16], F. Simeoni[23], G. I. Smirnov[9], A. Staude[12], A. Steinmetz[10], U. Stiegler[4], H. Stuhrmann[6], M. Szleper[26], K.M. Teichert[12], F. Tessarotto[23], W. Tlaczala[26], S. Trentalange[3], A. Tripet[12,16,t], G. Unel[2], M. Velasco[18,u], J. Vogt[12], R. Voss[4], R. Weinstein[8], C. Whitten[3], R. Windmolders[11], R. Willumeit[6], W. Wislicki[26], A. Witzmann[5,C] A. Yañez[21], Y. Ylöstalo[7], A.M. Zanetti[23], K. Zaremba[27], J. Zhao[6,D]

[1] University of Bielefeld, Physics Department, 33501 Bielefeld, Germany[aa]
[2] Bogaziçi University and Istanbul Technical University, Istanbul, Turkey[bb]
[3] University of California, Department of Physics, Los Angeles, CA 90024, USA[cc]
[4] CERN, 1211 Geneva 23, Switzerland
[5] University of Freiburg, Physics Department, 79104 Freiburg, Germany[aa]
[6] GKSS, 21494 Geesthacht, Germany[aa]
[7] Helsinki University of Technology, Low Temperature Laboratory and Institute of Particle Physics Technology, 02150 Espoo, Finland
[8] University of Houston, Department of Physics, Houston, TX 77204-5504, and Institute for Beam Particle Dynamics, Houston, TX 77204-5506, USA[cc,dd]
[9] JINR, Laboratory of Particle Physics, RU-141980 Dubna, Russia
[10] University of Mainz, Institute for Nuclear Physics, 55099 Mainz, Germany[aa]
[11] University of Mons, Faculty of Science, 7000 Mons, Belgium
[12] University of Munich, Physics Department, 80799 Munich, Germany[aa]
[13] Nagoya University, CIRSE, Furo-Cho, Chikusa-Ku, 464 Nagoya, Japan[ee]
[14] Nagoya University, Department of Physics, Furo-Cho, Chikusa-Ku, 464 Nagoya, Japan[ee]
[15] Nagoya University, College of Medical Technology, Daikominami 1, Higashi-Ku, 461 Nagoya, Japan[ee]
[16] NIKHEF, Delft University of Technology, FOM and Free University, 1009 AJ Amsterdam, The Netherlands[ff]
[17] Northeastern University, Department of Physics, Boston, MA 02115, USA[dd]
[18] Northwestern University, Department of Physics, Evanston, IL 60208, USA[cc,dd]
[19] Rice University, Bonner Laboratory, Houston, TX 77251-1892, USA[cc]
[20] CEA Saclay, DAPNIA, 91191 Gif-sur-Yvette, France[gg]
[21] University of Santiago de Compostela, Instituto de Fisica de Altas Energias, 15706 Santiago de Compostela, Spain[hh]
[22] Tel Aviv University, School of Physics, 69978 Tel Aviv, Israel[ii]
[23] INFN Trieste and University of Trieste, Department of Physics, 34127 Trieste, Italy
[24] Uppsala University, Department of Radiation Sciences, 75121 Uppsala, Sweden
[25] University of Virginia, Department of Physics, Charlottesville, VA 22901, USA[cc]
[26] Soltan Institute for Nuclear Studies and Warsaw University, 00681 Warsaw, Poland[jj]
[27] Warsaw University of Technology, 00681 Warsaw, Poland[jj]
[28] Yale University, Department of Physics, New Haven, CT 06511, USA[cc]
[a] Now at Gammadata, Uppsala, Sweden
[b] Also at Institut für Hochenergiephysik, 15738 Zeuthen, Germany; now at INFN Torino, I 10125 Torino, Italy
[c] Now at Thomas Jefferson National Laboratory, Newport News, VA 23606, USA
[d] Now at Ericsson Infocom AB, Sweden
[e] Now at University of Montreal, PQ, H3C 3J7, Montreal, Canada
[f] Now at DPhNC, University of Geneva, Geneva, Switzerland
[g] Now at University of Virginia, Department of Physics, Charlottesville, VA 22901, USA
[h] Now at INFN Trieste, 34127 Trieste, Italy
[i] Now at Fermi National Accelerator Laboratory, Batavia, IL 60510, USA
[j] Now at University of Wisconsin, Madison, WI 53706, USA
[k] Now at Stanford Linear Accelerator Center, Stanford, CA 94309, USA
[l] Now at Yale University, Department of Physics, New Haven, CT 06511, USA
[m] Permanent address: Miyazaki University, Faculty of Engineering, 889-21 Miyazaki-Shi, Japan

Measurements of the spin-dependent structure function g_1 of the deuteron are an important tool to study the internal spin structure of the nucleon. In combination with similar measurements on proton targets, they allow us to investigate the spin structure of the neutron and to verify the Bjorken sum rule [1].

In this paper, we report on a new measurement of $g_1^{\rm d}$, obtained by scattering longitudinally polarized muons of 190 GeV energy on longitudinally polarized deuterons in the kinematic range $0.0008 < x < 0.7$ and $0.2\ {\rm GeV}^2 < Q^2 < 100\ {\rm GeV}^2$. The data were collected in 1995 with the high-energy muon beam M2 of the CERN SPS. They complement earlier data taken in 1992 with a 100 GeV beam [2] and in 1994 with a 190 GeV beam [3], approximately doubling the data sample of our previous measurements with polarized deuterons. Out of 150 days of running time, 20 days were devoted to a measurement of the transverse virtual-photon nucleon asymmetry $A_2^{\rm d}$ with a transversely polarized target, using a beam of the same energy and polarization. In Ref. [4], we give a detailed account of our measurements of the spin structure of the proton; these results are used in the present paper to evaluate the structure function g_1 of the neutron and to test the Bjorken sum rule. Recent measurements of $g_1^{\rm p}$, $g_1^{\rm d}$, $A_2^{\rm p}$ and $A_2^{\rm d}$ from deep-inelastic electron scattering have also been reported by the E143 Collaboration at SLAC [5, 6, 7, 8].

The experimental set-up, the data taking procedure, and the evaluation of the cross-

[n] Permanent address: Paul Scherrer Institut, 5232 Villigen, Switzerland
[o] Now at Institute of Physical and Chemical Research (RIKEN), Wako 351-01, Japan
[p] Permanent address: University of California, Institute of Particle Physics, Santa Cruz, CA 95064, USA
[q] Permanent address: KEK, Tsukuba-Shi, 305 Ibaraki-Ken, Japan
[r] Bogoliubov Laboratory for Theoretical Physics, JINR, 141980 Dubna, Russia
[s] Now at Ericsson Telecommunication, 5120 AA Rijen, The Netherlands
[t] Now at University of Bielefeld, Physics Department, 33501 Bielefeld, Germany
[u] Now at CERN, 1211 Geneva 23, Switzerland
[v] Permanent address: University of Buenos Aires, Physics Department, 1428 Buenos Aires, Argentina
[w] Permanent address: The American University, Washington D.C. 20016, USA
[x] Now at University of Buenos Aires, Physics Department, 1428 Buenos Aires, Argentina
[y] Now at DESY, 22603 Hamburg, Germany
[z] Now at Dresden Technical University, 01062 Dresden, Germany
[A] Permanent address: Brookhaven National Laboratory, Upton, NY 11973, USA
[B] Present address: ESRF, F-38043 Grenoble, France
[C] Now at Hoffmann-La Roche GmbH, CH-4070 Basel, Switzerland
[D] Now at Los Alamos National Laboratory, Los Alamos, NM 87545, USA

[aa] Supported by the Bundesministerium für Bildung, Wissenschaft, Forschung und Technologie
[bb] Partially supported by TUBITAK and the Centre for Turkish-Balkan Physics Research and Application (Bogaziçi University)
[cc] Supported by the U.S. Department of Energy
[dd] Supported by the U.S. National Science Foundation
[ee] Supported by Monbusho Grant-in-Aid for Scientific Research (International Scientific Research Program and Specially Promoted Research)
[ff] Supported by the National Science Foundation (NWO) of the Netherlands
[gg] Supported by the Commissariat à l'Energie Atomique
[hh] Supported by the Comision Interministerial de Ciencia y Tecnologia (CICYT) and by the Xunta de Galicia
[ii] Supported by the Israel Science Foundation
[jj] Supported by KBN SPUB/P3/209/94 and SPUB/P3/112/95

[†] Deceased

section asymmetries

$$A_{\parallel}^{\mathrm{d}} = \frac{\sigma^{\uparrow\downarrow} - \sigma^{\uparrow\uparrow}}{\sigma^{\uparrow\downarrow} + \sigma^{\uparrow\uparrow}}, \qquad A_{\perp}^{\mathrm{d}} = \frac{\sigma^{\downarrow\rightarrow} - \sigma^{\uparrow\rightarrow}}{\sigma^{\downarrow\rightarrow} + \sigma^{\uparrow\rightarrow}} \tag{1}$$

for parallel, antiparallel and transverse configurations of beam and target polarizations, are similar to those of our previous measurements [3, 4, 9]. The beam polarization was determined by measuring the cross-section asymmetry for the scattering of polarized muons on polarized atomic electrons [4, 10]. For the beam of 190 GeV nominal energy, the average energy at the interaction vertex is 188 GeV and the polarization $P_\mu = -0.77 \pm 0.03$[1)]. In the evaluation of the deep-inelastic cross-section asymmetries of Eq. (1), the dependence of the polarization on the incoming muon energy is taken into account on an event-by-event basis.

The accuracy of the target polarization measurement [11] was improved with the help of a new NMR coil arrangement; typical longitudinal deuteron polarizations were $P_{\mathrm{d}} = \pm 0.50$, with an overall accuracy of $\Delta P_{\mathrm{d}}/P_{\mathrm{d}} = 2.1\%$. For the runs with a transversely polarized target, the average deuteron polarization was $P_{\mathrm{d}} = \pm 0.43$, with the same error.

The asymmetries $A_{\parallel}^{\mathrm{d}}$ and $A_{\perp}^{\mathrm{d}}$ of Eq. (1) are related to virtual-photon deuteron asymmetries A_1^{d} and A_2^{d} and to the spin-dependent structure functions g_1^{d} and g_2^{d} by

$$A_{\parallel}^{\mathrm{d}} = D(A_1^{\mathrm{d}} + \eta A_2^{\mathrm{d}}), \qquad A_{\perp}^{\mathrm{d}} = d(A_2^{\mathrm{d}} - \xi A_1^{\mathrm{d}}) \tag{2}$$

and

$$g_1^{\mathrm{d}} = \frac{F_2^{\mathrm{d}}}{2x(1+R)}(A_1^{\mathrm{d}} + \gamma A_2^{\mathrm{d}}), \qquad g_2^{\mathrm{d}} = \frac{F_2^{\mathrm{d}}}{2x(1+R)}\left(\frac{A_2^{\mathrm{d}}}{\gamma} - A_1^{\mathrm{d}}\right). \tag{3}$$

We neglect the contribution from quadrupole structure functions which is expected to be small in the kinematic range of our data [12, 13]. The coefficients η, γ, and ξ depend only on kinematic variables; the depolarization factors D and d depend, in addition, on the unpolarized structure function $R = \sigma_{\mathrm{L}}/\sigma_{\mathrm{T}}$ [14, 15].

The virtual-photon deuteron asymmetries are defined as $A_1^{\mathrm{d}} = \frac{1}{2}(\sigma_0^{\mathrm{T}} - \sigma_2^{\mathrm{T}})/\sigma_{\mathrm{T}}$, $A_2^{\mathrm{d}} = \frac{1}{2}(\sigma_0^{\mathrm{TL}} + \sigma_1^{\mathrm{TL}})/\sigma_{\mathrm{T}}$ [13, 16]. Here, $\sigma_{\mathrm{T}} = \frac{1}{3}(\sigma_0^{\mathrm{T}} + \sigma_1^{\mathrm{T}} + \sigma_2^{\mathrm{T}})$ is the total transverse photoabsorption cross-section, σ_J^{T} is the cross section for absorption of a virtual photon by a deuteron with total spin projection J in the photon direction, and σ_J^{TL} results from the spin-flip amplitude in forward photon-deuteron Compton scattering.

We first evaluate A_2^{d} from the measurement of $A_{\perp}^{\mathrm{d}}$, using a parametrization of $A_{\parallel}^{\mathrm{d}}$. This analysis is similar to the one described in Ref. [9] and the result is shown in Table 1 and in Fig. 1a. It is compatible with zero and much smaller than the positivity bound $|A_2| \leq \sqrt{R}$ [17]. This asymmetry has also been measured in the SLAC E143 experiment with better statistical accuracy, but in a more limited x range and at a smaller average Q^2. Since the Q^2 dependence of A_2 is unknown, an assumption must be made in order to compare the two measurements. From Eqs (3):

$$A_2 = \gamma\frac{g_1 + g_2}{F_1} = \frac{2Mx}{\sqrt{Q^2}}\frac{g_1 + g_2}{F_1}. \tag{4}$$

Since g_1/F_1 is Q^2-independent within the errors, we make the same hypothesis for $(g_1 + g_2)/F_1$ and use Eq. (4) to evaluate our and the SLAC data at a common $Q^2 = 5$ GeV^2. The results are in good agreement in the x region of overlap (Fig. 1b).

[1)] The beam of 100 GeV nominal energy has an average energy at the interaction vertex of 99.4 GeV and the polarization obtained with the same method is $P_\mu = -0.81 \pm 0.03$.

The evaluation of the asymmetry $A_1^{\rm d}$ and of the structure function $g_1^{\rm d}$ is also similar to that of our 1994 data [3]. Since, in the kinematic region of this measurement, η and γ are small and the asymmetry $A_2^{\rm d}$ is compatible with zero, we neglect the terms proportional to $A_2^{\rm d}$ in Eq. (3), such that

$$A_1^{\rm d} = (1+\gamma^2)\frac{g_1^{\rm d}}{F_1^{\rm d}} = 2x(1+R)\frac{g_1^{\rm d}}{F_2^{\rm d}}. \qquad (5)$$

The systematic uncertainty due to a possible residual $A_2^{\rm d}$ contribution is estimated from both our and the SLAC results.

The analysis is limited to the kinematic region with $x \geq 0.0008$ and $Q^2 \geq 0.2$ GeV^2; data with $Q^2 < 1$ GeV^2 are presented here for the first time. Cuts are applied to restrict the inelasticity to $y \leq 0.9$, the scattering angle to $\Theta \geq 2$ mrad, the energy of the scattered muon to $E'_\mu \geq 19$ GeV, and the energy transfer to the target to $\nu \geq 15$ GeV. After these cuts, 11.2×10^6 events remain for the final analysis from the new measurement. The 1992 and 1994 data were also reanalysed to account for the improved measurement of the beam polarization, and for a new parametrization of the unpolarized structure function $F_2(x,Q^2)$ [18]. The treatment of radiative corrections to convert the measured cross-section asymmetries to single-photon asymmetries [19, 20] has also been improved. For reasons detailed in Ref. [4], the new procedure increases the statistical errors of $A_1^{\rm d}$, in particular at small x.

The new results for $Q^2 \geq 1$ GeV^2 are in agreement with the 1992 and 1994 data within the statistical errors and we combine them for the subsequent analysis. The combined results for $A_1^{\rm d}$ are shown as a function of x and Q^2 in Table 2 and Fig. 2. In this figure, we also compare our results to the SLAC E143 measurement at smaller Q^2. The data confirm earlier observations that no Q^2 dependence of A_1 is visible within the accuracy of the present data [7]. The Q^2-averaged results for $A_1^{\rm d}(x)$ are shown in Fig. 3. The new results for $Q^2 \geq 1$ GeV^2 are compared to our 1992 and 1994 data in Fig. 3a and the combined results are shown in Fig. 3b together with the small-Q^2 results; the new data do not confirm our previous observation that $A_1^{\rm d}(x)$ is negative at small x. The dominant systematic errors at small x are due to time-dependent variations of the acceptance ratio for events from the upstream and downstream target cells, and to uncertainties in $A_2^{\rm d}$ and radiative corrections. At large x, the dominant sources of systematic errors are uncertainties of the beam and target polarizations, and of R. To compute the total systematic error, the individual contributions are combined in quadrature.

The structure function $g_1^{\rm d}(x)$ is obtained from Eq. (5) using the NMC parametrization of $F_2^{\rm d}$ [18] and the SLAC parametrization of R [21]. The use of the SLAC parametrization of R requires an extrapolation to small x and Q^2 where it is not constrained by experimental data. This causes, however, a negligible uncertainty since R-dependent terms nearly cancel in the evaluation of g_1 from $A_\parallel$. The resulting $g_1^{\rm d}(x)$ at the average Q^2 of each bin is shown in Table 3.

To test sum rule predictions for g_1, we use our data in the kinematic region $Q^2 \geq 1$ GeV^2, $x \geq 0.003$. For such tests, moments of structure functions must be evaluated at fixed values of Q^2. Although the asymmetry $A_1^{\rm d}$ and the ratio $g_1^{\rm d}/F_1^{\rm d}$ exhibit no Q^2 dependence within the errors, different Q^2 evolutions of g_1 and F_1 are expected from perturbative QCD.

We estimate the Q^2 dependence of $g_1^{\rm d}$ from the Altarelli–Parisi evolution equations [22, 23], using the QCD splitting and coefficient functions at next-to-leading order [24] and a program by Ball, Forte and Ridolfi [25]. Our results obtained from this

analysis refer to the Adler–Bardeen (AB) factorization scheme. They are similar to results recently obtained by other groups [26, 27]. The structure functions g_1 of the proton and the deuteron are decomposed into a polarized singlet quark distribution $\Delta\Sigma(x)$ and nonsinglet quark distributions $\Delta q_{\rm NS}^{\rm p}(x)$ and $\Delta q_{\rm NS}^{\rm d}(x)$. At next-to-leading order, the gluon distribution $\Delta g(x)$ also needs to be taken into account. These distributions are parametrised at a given Q^2 by

$$\Delta f_j(x) = \eta_j N x^{\alpha_j}(1-x)^{\beta_j}(1+a_j x), \tag{6}$$

where N is fixed by the normalization $\eta_j = \int_0^1 \Delta f_j(x){\rm d}x$. Following Ref. [25], we fix a_j to be the same for the singlet quark and gluon distributions. We also fix β_g to 4 as suggested by QCD counting rules [28] since this parameter is poorly constrained by the data. The parameters of the nonsinglet distributions are assumed to be equal except for the normalizations η_j, which are constrained by relating the moments of $\Delta q_{\rm NS}^{\rm p}$ and $\Delta q_{\rm NS}^{\rm d}$ to the flavour-SU(3) coupling constants F and D. For these coupling constants we used $F + D = g_{\rm A}/g_{\rm V} = 1.2573 \pm 0.0028$ [29] and $F/D = 0.575 \pm 0.016$ [30]. For the strong coupling constant, we use $\alpha_{\rm s}(m_{\rm Z}^2) = 0.118 \pm 0.003$ [29]. We fit the evolved parton distributions to the present deuteron data and to our proton data [4] in (x,Q^2) bins, to the earlier EMC proton results [14], and to the E143 measurements [5, 6, 7]. The EMC and E143 data were taken at the average Q^2 in each x bin. The χ^2 of the fit is 283.5 for 295 degrees of freedom and the fitted parameters are given in Table 4.

We obtain g_1 at a fixed Q_0^2 from

$$g_1(x,Q_0^2) = g_1(x,Q^2) + [g_1^{\rm fit}(x,Q_0^2) - g_1^{\rm fit}(x,Q^2)], \tag{7}$$

where $g_1^{\rm fit}$ is our fit, and where $g_1(x,Q^2)$ and $g_1^{\rm fit}(x,Q^2)$ are evaluated at the average Q^2 of each x bin. The resulting g_1 at $Q_0^2 = 10\,{\rm GeV}^2$, which is the average Q^2 of our data, is shown in Table 3. The errors of the QCD evolution are dominated by the uncertainties of the renormalization and factorization scales [25]. They also account for uncertainties of the heavy flavour thresholds, the error of $\alpha_{\rm s}$, and for the statistical and systematic errors of the input data. For a comparison to the SLAC data, we also evolve $g_1^{\rm d}$ from both experiments to $Q_0^2 = 5$ GeV^2 (Fig. 4a).

To obtain the spin-dependent structure function of the neutron $g_1^{\rm n}$ from our deuteron and proton data, we assume that in the kinematic range of our data ($x \leq 0.7$)

$$g_1^{\rm p} + g_1^{\rm n} = 2g_1^{\rm d}/(1-1.5\omega_D), \tag{8}$$

where $\omega_D = 0.05 \pm 0.01$ is the D-wave state probability of the deuteron [3]. The results are shown in Fig. 4b and confirm the earlier observation of a significant difference between the spin-dependent structure functions of the proton and the neutron at small x. A similar analysis has been presented by the E143 Collaboration [6]. More direct measurements of $g_1^{\rm n}$ with polarized ^{3}He targets have been made by the E142 [31] and E154 [32] experiments at SLAC and by the HERMES experiment at DESY [33]. The E142 and E143 results are also shown in Fig. 4b; all measurements are in agreement in the x range of overlap.

We evaluate the first moment of $g_1^{\rm d}$ at $Q_0^2 = 10$ GeV^2 which is the average Q^2 of our data (Table 3). From our combined deuteron results, the contribution from the measured x range is:

$$\int_{0.003}^{0.7} g_1^{\rm d}(x,Q_0^2){\rm d}x = 0.0407 \pm 0.0059 \pm 0.0035 \pm 0.0030 \qquad (Q_0^2 = 10\ {\rm GeV}^2), \tag{9}$$

where the first error is statistical, the second one is systematic and the third is an uncertainty due to the Q^2 evolution of $g_1^{\rm d}$. As in Refs. [3, 4], the contribution from the unmeasured region at small x is estimated by assuming $g_1^{\rm d}(x, Q_0^2) = constant$, where the constant is obtained by averaging the two data points with the smallest x. This correction amounts to $\int_0^{0.003} g_1^{\rm d}(x){\rm d}x = 0.0000 \pm 0.0009$. The error covers the general Regge dependence $g_1(x) \propto x^{-\alpha}$, with $-0.5 \leq \alpha \leq 0$ [34], but does not account for more divergent small-x behaviours of g_1. To estimate the contribution from the unmeasured region at large x, we assume $A_1^{\rm d} = 0.4 \pm 0.6$ which is consistent both with the data and with the bound $|A_1| \leq 1$, and find $\int_{0.7}^1 g_1^{\rm d}(x){\rm d}x = 0.0006 \pm 0.0009$. The first moment of $g_1^{\rm d}$ is thus:

$$\Gamma_1^{\rm d}(Q_0^2) = \int_0^1 g_1^{\rm d}(x, Q_0^2){\rm d}x = 0.0414 \pm 0.0059 \pm 0.0037 \pm 0.0030 \qquad (Q_0^2 = 10\ {\rm GeV}^2). \quad (10)$$

The contributions to the systematic error of this integral are detailed in Table 5. When we assume scaling of A_1, these integrals are $\int_{0.003}^{0.7} g_1^{\rm d}(x, Q_0^2){\rm d}x = 0.0374 \pm 0.0069 \pm 0.0039$ and $\Gamma_1^{\rm d}(Q_0^2) = 0.0372 \pm 0.0069 \pm 0.0041$, at the same $Q_0^2 = 10\,{\rm GeV}^2$.

The first moment $\Gamma_1^{\rm p} + \Gamma_1^{\rm n} = 2\Gamma_1^{\rm d}/(1 - 1.5\omega_D)$ allows us to determine the flavour-singlet axial charge $a_0(Q^2)$ of the nucleon. This analysis relies on ${\rm SU}(3)_f$ relations for the axial vector coupling constants within the baryon octet [35] which are completely determined by the two constants F and D. Perturbative QCD corrections [36] were calculated for three quark flavours, assuming $\alpha_{\rm s}(Q^2 = 10\ {\rm GeV}^2) = 0.249 \pm 0.015$ corresponding to $\alpha_{\rm s}(m_{\rm Z}^2) = 0.118 \pm 0.003$ as used earlier. Neglecting contributions from polarized charm quarks we obtain from Eq. (10)

$$a_0 = a_{\rm u} + a_{\rm d} + a_{\rm s} = 0.30 \pm 0.08 \qquad (Q_0^2 = 10\ {\rm GeV}^2), \quad (11)$$

where the $a_{\rm q}$ are the axial charges of the individual quark flavours, and

$$a_{\rm s} = -0.09 \pm 0.03 \qquad (Q_0^2 = 10\ {\rm GeV}^2). \quad (12)$$

These results are at variance with the Ellis–Jaffe assumption of $a_{\rm s} = 0$ and the prediction $a_0 = 3F - D = 0.579 \pm 0.025$ [35]. The Ellis–Jaffe sum rule predicts $\Gamma_1^{\rm d} = 0.071 \pm 0.003$ at $Q_0^2 = 10\ {\rm GeV}^2$, which is 3.7 standard deviations above our measurement. The value of $a_{\rm s}$ and the violation the Ellis–Jaffe sum rule depend on the assumption of ${\rm SU}(3)_f$ symmetry, whereas it has been shown that the value of a_0 is largely insensitive to possible ${\rm SU}(3)_f$ breaking effects [37].

The axial charge a_0 and the corresponding charges of the individual quark flavours can be understood as quark contributions to the proton spin, up to a gluonic contribution which is due to the $U(1)$ anomaly of the singlet axial vector current [38]. In the Adler–Bardeen scheme, the axial charges are decomposed into quark and gluon contributions Δq and Δg as

$$a_{\rm q} = \Delta q - \frac{\alpha_{\rm s}}{2\pi}\Delta g \qquad (q = u,\ d,\ s). \quad (13)$$

The axial charge $a_{\rm q}$ depends on Q^2, whereas Δq is Q^2-independent in the AB scheme. This suggests to interpret Δq as the intrinsic quark-spin content of the nucleon. When we make the assumption that $\Delta s = 0$, our measurement of a_0 corresponds to a gluon polarization $\Delta g = 2.3 \pm 0.7$ at $Q^2 = 10\ {\rm GeV}^2$ in the AB scheme. From the QCD analysis discussed in this paper, the first moment of the polarized gluon distribution obtained at $10\ {\rm GeV}^2$ using the parton distributions of Table 4 is $\Delta g \approx 2$.

To test the Bjorken sum rule [1], we combine the present result for $\Gamma_1^{\rm d}$ with our earlier result $\Gamma_1^{\rm p} = 0.136 \pm 0.013 \pm 0.009 \pm 0.005$ at $Q_0^2 = 10\,{\rm GeV}^2$ [4]. Taking into account correlations between errors [39], we obtain $\Gamma_1^{\rm n} = -0.046 \pm 0.018 \pm 0.014 \pm 0.012$ and

$$\Gamma_1^{\rm p} - \Gamma_1^{\rm n} = 0.183 \pm 0.029 \pm 0.018 \pm 0.007 \qquad (Q_0^2 = 10\ {\rm GeV}^2). \tag{14}$$

The Bjorken prediction at $Q_0^2 = 10\ {\rm GeV}^2$, including perturbative QCD corrections up to third order in α_s [40] and assuming three quark flavours, is

$$\Gamma_1^{\rm p} - \Gamma_1^{\rm n} = 0.186 \pm 0.002 \qquad (Theory, Q_0^2 = 10\ {\rm GeV}^2) \tag{15}$$

in agreement with our result.

We also determine $\Gamma_1^{\rm d}$ by combining results on $A_1^{\rm d}$ from this and from the E143 experiment. We evaluate $g_1^{\rm d}$ at a common $Q_0^2 = 5\ {\rm GeV}^2$, using the same parametrizations of $F_2^{\rm d}(x,Q^2)$ and $R(x,Q^2)$ and the same Q^2 evolution procedure as above. We obtain $\Gamma_1^{\rm d} = 0.039 \pm 0.004 \pm 0.004 \pm 0.004$, corresponding to $a_0 = 0.28 \pm 0.07$ and $a_{\rm s} = -0.10 \pm 0.03$.

In summary, we have presented a new measurement of the spin-dependent structure function $g_1^{\rm d}$ from polarized deep inelastic muon-deuteron scattering. This measurement confirms our earlier observation of an important difference between $g_1^{\rm p}$ and $g_1^{\rm n}$ at small x. The results are in good agreement with our previous data and we combine them for the final analysis. Our measurement of the first moment $\Gamma_1^{\rm d}$ disagrees with the Ellis–Jaffe prediction by 3.7 standard deviations; the flavour-singlet axial charge of the nucleon is $a_0 = 0.30 \pm 0.08$. Assuming ${\rm SU}(3)_f$ symmetry, we find a singlet axial charge of the strange quark $a_{\rm s} = -0.09 \pm 0.03$. Our results for Γ_1 of the proton and the deuteron confirm the Bjorken sum rule.

References

[1] J.D. Bjorken, Phys. Rev. 148 (1966) 1467; Phys. Rev. D1 (1970) 1376.
[2] SMC, B. Adeva et al., Phys. Lett. B302 (1993) 533.
[3] SMC, D. Adams et al., Phys. Lett. B357 (1995) 248.
[4] SMC, D. Adams et al., *Spin Structure of the Proton from Polarized Deep Inelastic Muon-Proton Scattering*, to be submitted to Phys. Rev. D.
[5] E143 Collaboration, K. Abe et al., Phys. Rev. Lett. 74 (1995) 346.
[6] E143 Collaboration, K. Abe et al., Phys. Rev. Lett. 75 (1995) 25.
[7] E143 Collaboration, K. Abe et al., Phys. Lett. B364 (1995) 61.
[8] E143 Collaboration, K. Abe et al., Phys. Rev. Lett. 76 (1996) 587.
[9] SMC, D. Adams et al., Phys. Lett. B336 (1994) 125.
[10] P. Schüler, Proc. 8th Int. Symposium on High Energy Spin Physics, Minneapolis 1988, ed. by K.J. Heller, AIP Conference Proceedings Vol. 187.
[11] SMC, B. Adeva et al., Nucl. Instrum. Methods A343 (1994) 363.
[12] H. Khan and P. Hoodbhoy, Phys.Lett. B298 (1993) 181.
[13] P. Hoodbhoy, R.L. Jaffe and A. Manohar, Nucl. Phys. B312 (1989) 571.
[14] EMC, J. Ashman et al., Phys. Lett. B206 (1988) 364; Nucl. Phys. B328 (1989) 1.
[15] T. Pussieux and R. Windmolders, in: *Internal Spin Structure of the Nucleon*, ed. by V.W. Hughes and C. Cavata (World Scientific, Singapore, 1995), p. 212.
[16] M.A. Rodriguez, Ph.D. Thesis, University of Santiago de Compostela, 1994.
[17] M.G. Doncel and E. de Rafael, Nuovo Cimento 4A (1971) 363; P. Gnädig and F. Niedermayer, Nucl. Phys. B55 (1973) 612.
[18] NMC, M. Arneodo et al., Phys. Lett. B364 (1995) 107.

[19] T.V. Kukhto and N.M. Shumeiko, Nucl. Phys. B219 (1983) 412.
[20] I.V. Akushevich and N.M. Shumeiko, J. Phys. G20 (1994) 513.
[21] L.W. Whitlow et al., Phys. Lett. B250 (1990) 193. We use the parametrisation published in L.W. Whitlow, PhD Thesis, Stanford University, 1990.
[22] G. Altarelli and G. Parisi, Nucl.Phys. B126 (1977) 298.
[23] G. Altarelli, Phys. Rep. 81 (1982) 1.
[24] R. Mertig and W.L. van Neerven, Leiden preprint INLO-PUB-6/95, hep-ph/9506451; W. Vogelsang, Phys. Rev. D54 (1996) 2023.
[25] R. D. Ball, S. Forte, and G. Ridolfi, Phys. Lett. B378 (1996) 255.
[26] M. Glück et al., Phys Rev. D53 (1996) 4775.
[27] T. Gehrmann and W.J. Stirling, Phys. Rev. D53 (1996) 6100.
[28] S.J. Brodsky, M. Burkardt and I. Schmidt, Nucl. Phys. B441 (1995) 197.
[29] Particle Data Group, R.M. Barnett et al., Phys. Rev. D54 (1996) 1.
[30] F.E. Close and R.G. Roberts, Phys. Lett. B316 (1993) 165.
[31] E142, P.L. Anthony et al., Phys. Rev. Lett. 71 (1993) 959; Phys. Rev. D54 (1996) 6620.
[32] E. Hughes, Proc. 28th Int. Conference on High Energy Physics, Warsaw 1996, to be published.
[33] A. Simon, Proc. 12th Int. Symposium on High-Energy Spin Physics, Spin96, Amsterdam 1996, to be published.
[34] R.L. Heimann, Nucl. Phys. B64 (1973) 429; J. Ellis and M. Karliner, Phys. Lett. B213 (1988) 73.
[35] J. Ellis and R.L. Jaffe, Phys. Rev. D9 (1974) 1444; D10 (1974) 1669.
[36] S.A. Larin, Phys. Lett. B334 (1994) 192.
[37] J. Lichtenstadt and H.J. Lipkin, Phys. Lett. B353 (1995) 119.
[38] G. Altarelli and G.G. Ross, Phys. Lett. B212 (1988) 391; R.D. Carlitz, J.C. Collins and A.H. Mueller, Phys. Lett. B214 (1988) 229; S. Forte, CERN-TH.7453/94 (1994) (hep-ph/9409416), and references therein.
[39] J.J. Saborido, Ph.D. Thesis, University of Santiago de Compostela, 1995; J.J. Saborido, SMC Internal Note 95-32, 1995 (unpublished).
[40] S.A. Larin and J.A.M. Vermaseren, Phys. Lett. B259 (1991) 345.

Table 1: The transverse virtual-photon asymmetry A_2^d in intervals of x. Only statistical errors are shown.

x range	$\langle x \rangle$	$\langle Q^2 \rangle$ (GeV^2)	A_2^{d}
$0.0015 - 0.0050$	0.0029	0.8	0.011 ± 0.068
$0.0050 - 0.0200$	0.0108	2.6	-0.029 ± 0.055
$0.0200 - 0.0500$	0.0333	6.4	0.145 ± 0.069
$0.0500 - 0.1200$	0.0801	10.9	0.110 ± 0.083
$0.1200 - 0.6000$	0.2280	18.0	-0.017 ± 0.110

Table 2: The virtual-photon deuteron cross section asymmetry A_1^{d} obtained from the combined SMC deuteron data. The errors are statistical only.

$\langle x \rangle$	$\langle Q^2 \rangle$ (GeV^2)	A_1	$\langle x \rangle$	$\langle Q^2 \rangle$ (GeV^2)	A_1
0.0009	0.25	-0.058 ± 0.055	0.0341	3.18	-0.056 ± 0.148
0.0010	0.30	0.004 ± 0.067	0.0343	3.75	0.063 ± 0.153
0.0011	0.34	0.056 ± 0.084	0.0342	4.54	-0.158 ± 0.099
0.0014	0.38	-0.045 ± 0.041	0.0342	5.80	-0.040 ± 0.063
0.0017	0.46	-0.088 ± 0.050	0.0344	7.79	0.038 ± 0.042
0.0018	0.55	0.013 ± 0.055	0.0359	10.13	-0.020 ± 0.049
0.0023	0.58	0.114 ± 0.042	0.0476	2.89	0.292 ± 0.155
0.0025	0.70	-0.099 ± 0.046	0.0478	4.31	0.120 ± 0.101
0.0028	0.82	-0.056 ± 0.051	0.0478	5.83	0.055 ± 0.077
0.0032	0.70	0.099 ± 0.114	0.0480	7.82	0.111 ± 0.048
0.0035	0.90	0.066 ± 0.035	0.0484	10.96	0.093 ± 0.035
0.0043	1.14	0.005 ± 0.028	0.0528	14.71	-0.017 ± 0.051
0.0051	1.43	-0.019 ± 0.035	0.0744	2.94	-0.042 ± 0.245
0.0056	1.70	0.051 ± 0.060	0.0745	4.33	-0.005 ± 0.154
0.0077	1.16	-0.006 ± 0.083	0.0744	5.82	0.046 ± 0.117
0.0071	1.47	0.077 ± 0.055	0.0748	7.85	0.021 ± 0.067
0.0072	1.76	-0.061 ± 0.039	0.0754	11.05	0.101 ± 0.045
0.0076	2.04	-0.073 ± 0.037	0.0760	16.32	-0.022 ± 0.036
0.0084	2.34	0.040 ± 0.044	0.0855	23.07	-0.005 ± 0.055
0.0090	2.63	0.047 ± 0.056	0.1193	3.99	0.219 ± 0.251
0.0096	2.93	0.030 ± 0.086	0.1196	7.39	0.064 ± 0.111
0.0124	1.40	-0.097 ± 0.093	0.1199	11.12	0.013 ± 0.079
0.0134	1.76	-0.018 ± 0.091	0.1205	16.42	0.084 ± 0.058
0.0132	2.06	0.029 ± 0.077	0.1206	24.83	0.080 ± 0.053
0.0129	2.36	-0.057 ± 0.064	0.1292	34.25	0.085 ± 0.073
0.0126	2.66	-0.005 ± 0.054	0.1709	9.67	0.235 ± 0.109
0.0126	2.96	-0.037 ± 0.047	0.1714	16.46	0.052 ± 0.094
0.0132	3.30	-0.065 ± 0.039	0.1716	24.83	0.264 ± 0.085
0.0146	3.74	-0.042 ± 0.039	0.1715	34.91	0.055 ± 0.092
0.0165	4.43	-0.024 ± 0.035	0.1769	45.38	0.349 ± 0.103
0.0184	5.43	0.007 ± 0.057	0.2368	10.01	0.252 ± 0.144
0.0236	2.12	-0.089 ± 0.115	0.2385	16.52	0.223 ± 0.115
0.0239	2.82	0.085 ± 0.097	0.2394	24.84	0.078 ± 0.101
0.0243	3.30	-0.060 ± 0.112	0.2392	34.92	0.308 ± 0.110
0.0239	3.76	-0.022 ± 0.094	0.2454	52.68	0.309 ± 0.075
0.0237	4.54	-0.075 ± 0.051	0.3396	19.73	0.121 ± 0.131
0.0241	5.76	0.003 ± 0.036	0.3426	55.93	0.205 ± 0.095
0.0263	7.41	0.021 ± 0.041	0.4730	25.80	0.398 ± 0.174
0.0341	2.38	-0.079 ± 0.184	0.4830	71.65	0.321 ± 0.135

Table 3: The spin-dependent structure function $g_1^{\rm d}$. The first error is statistical, the second one systematic. The third error in the last column is the uncertainty of the QCD evolution.

x range	$\langle x \rangle$	$\langle Q^2 \rangle$	A_1	g_1	$g_1(Q_0^2 = 10\,\mathrm{GeV}^2)$
0.003–0.006	0.005	1.3	0.001±0.021±0.002	0.02±0.50±0.06	0.19±0.50±0.06±0.46
0.006–0.010	0.008	2.0	−0.014±0.019±0.003	−0.23±0.31±0.04	−0.08±0.31±0.04±0.12
0.010–0.020	0.014	3.5	−0.033±0.016±0.003	−0.33±0.16±0.03	−0.24±0.16±0.03±0.05
0.020–0.030	0.025	5.5	−0.008±0.022±0.003	−0.05±0.14±0.02	−0.01±0.14±0.02±0.02
0.030–0.040	0.035	7.5	−0.011±0.026±0.003	−0.05±0.12±0.01	−0.04±0.12±0.01±0.01
0.040–0.060	0.049	10.1	0.076±0.023±0.006	0.26±0.08±0.02	0.26±0.08±0.02±0.00
0.060–0.100	0.077	14.4	0.020±0.023±0.003	0.04±0.05±0.01	0.03±0.05±0.01±0.01
0.100–0.150	0.122	20.6	0.074±0.030±0.006	0.09±0.04±0.01	0.08±0.04±0.01±0.01
0.150–0.200	0.172	26.6	0.188±0.043±0.015	0.15±0.04±0.01	0.15±0.04±0.01±0.01
0.200–0.300	0.241	34.0	0.250±0.046±0.018	0.123±0.022±0.008	0.124±0.022±0.008±0.004
0.300–0.400	0.342	43.6	0.181±0.077±0.014	0.044±0.019±0.003	0.051±0.019±0.003±0.002
0.400–0.700	0.479	54.4	0.354±0.106±0.027	0.031±0.009±0.002	0.040±0.009±0.002±0.003

Table 4: Parameters of the polarized parton distributions from the NLO QCD fit to $g_1^{\rm d}$ and $g_1^{\rm p}$ discussed in the text, at $Q^2 = 1\,\mathrm{GeV}^2$. The parameter a_j is constrained to be the same for $\Delta\Sigma(x)$ and $\Delta g(x)$. The normalizations η_j for the non-singlet distributions $\Delta q_{\rm NS}^{\rm d}(x)$ and $\Delta q_{\rm NS}^{\rm p}(x)$ are determined by the axial vector coupling constants F and D.

	η_j	α_j	β_j	a_j
$\Delta q_{\rm NS}^{\rm d,p}(x)$	—	-0.7 ± 0.3	2.1 ± 0.3	25 ± 39
$\Delta\Sigma(x)$	0.40 ± 0.04	0.7 ± 0.3	1.6 ± 1.0	-1.3 ± 0.2
$\Delta g(x)$	1.0 ± 0.6	-0.7 ± 0.3	4 (fixed)	$a_{\Delta\Sigma}$

Table 5: Contributions to the error on $\Gamma_1^{\rm d}$ at $Q_0^2 = 10$ GeV^2

Error source	$\Delta\Gamma_1^{\rm d}$
Beam polarization	0.0015
Acceptance variation	0.0014
Momentum calibration	0.0014
Target polarization	0.0013
Uncertainty on F_2	0.0012
Kinematic resolution	0.0010
Extrapolation at low x	0.0009
Extrapolation at high x	0.0009
Radiative corrections	0.0008
Dilution factor	0.0006
Proton background	0.0006
Neglect of A_2	0.0005
Total systematic error	0.0037
QCD evolution	0.0030
Statistical error	0.0059

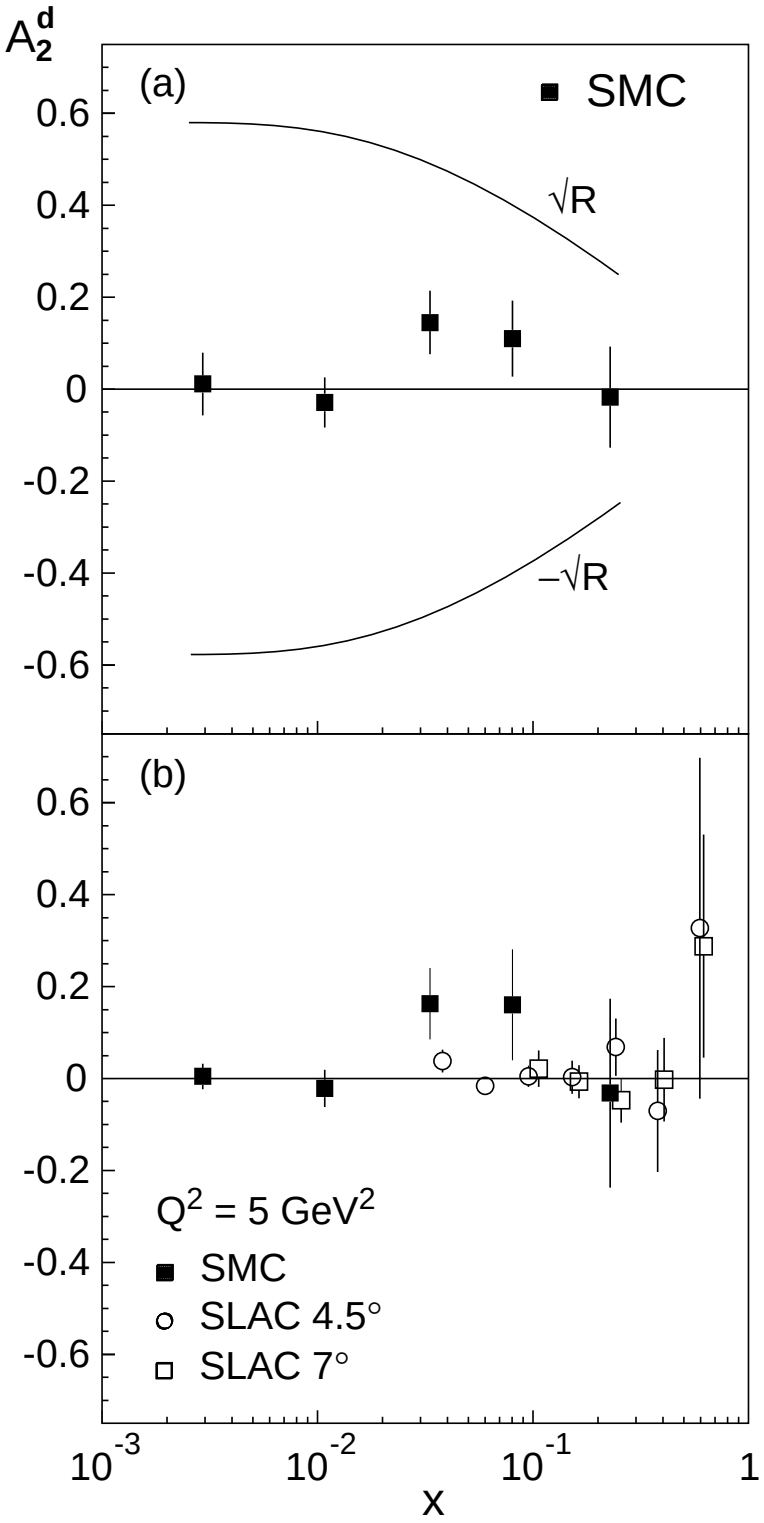

Figure 1: The virtual-photon deuteron cross section asymmetry $A_2^{\rm d}$ as a function of the scaling variable x. In (a), $A_2^{\rm d}$ is shown at the average Q^2 of each x bin. Only statistical errors are shown; the systematic errors are estimated to be much smaller. In (b), results from the present measurement are compared to results from the SLAC E143 experiment [8] at a common $Q^2 = 5$ GeV^2. Errors are statistical.

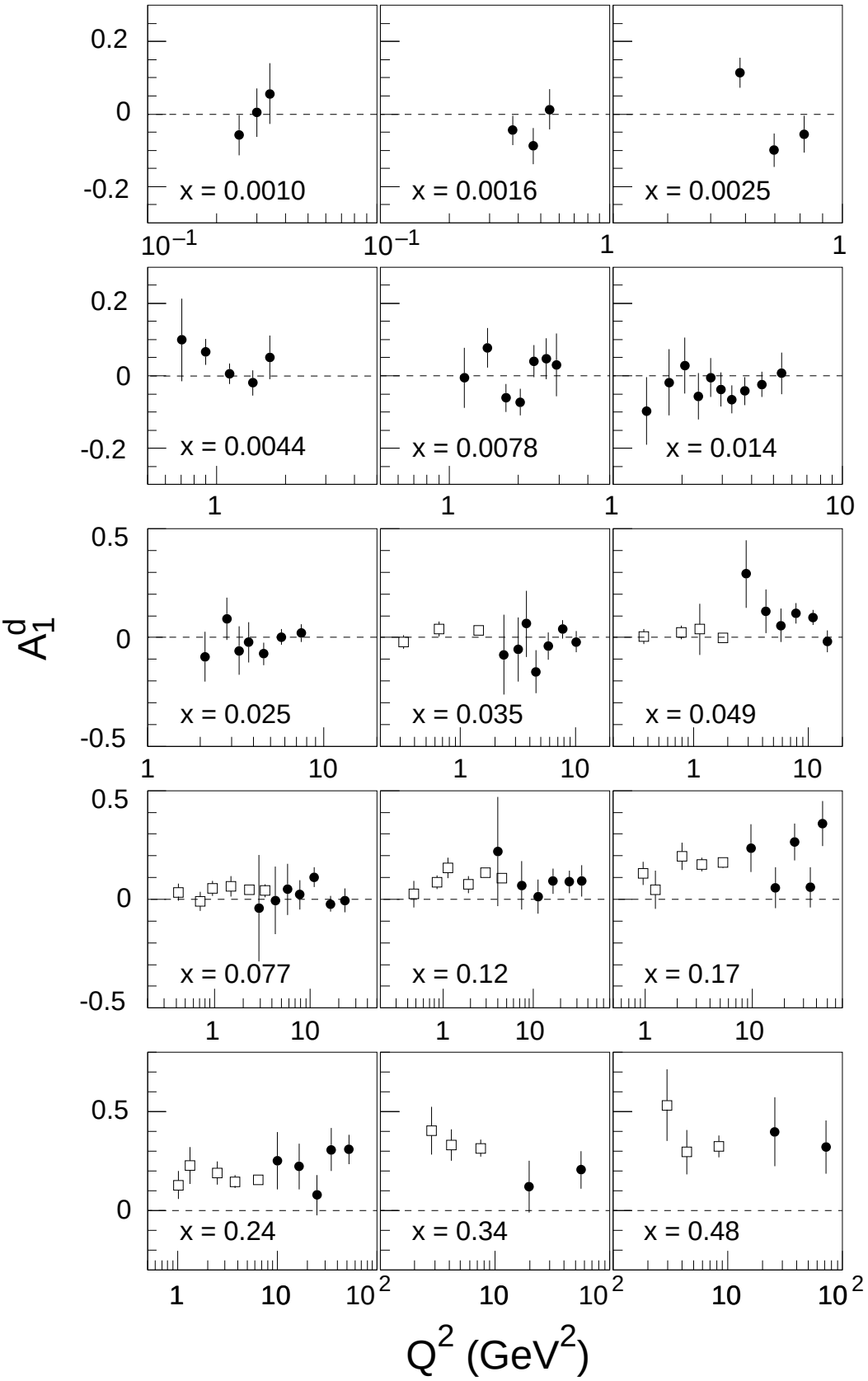

Figure 2: The virtual-photon deuteron asymmetry $A_1^{\rm d}$ as a function of the scaling variable x and four-momentum transfer Q^2. Also shown by open symbols are results from the SLAC E143 experiment [7]. Only statistical errors are shown.

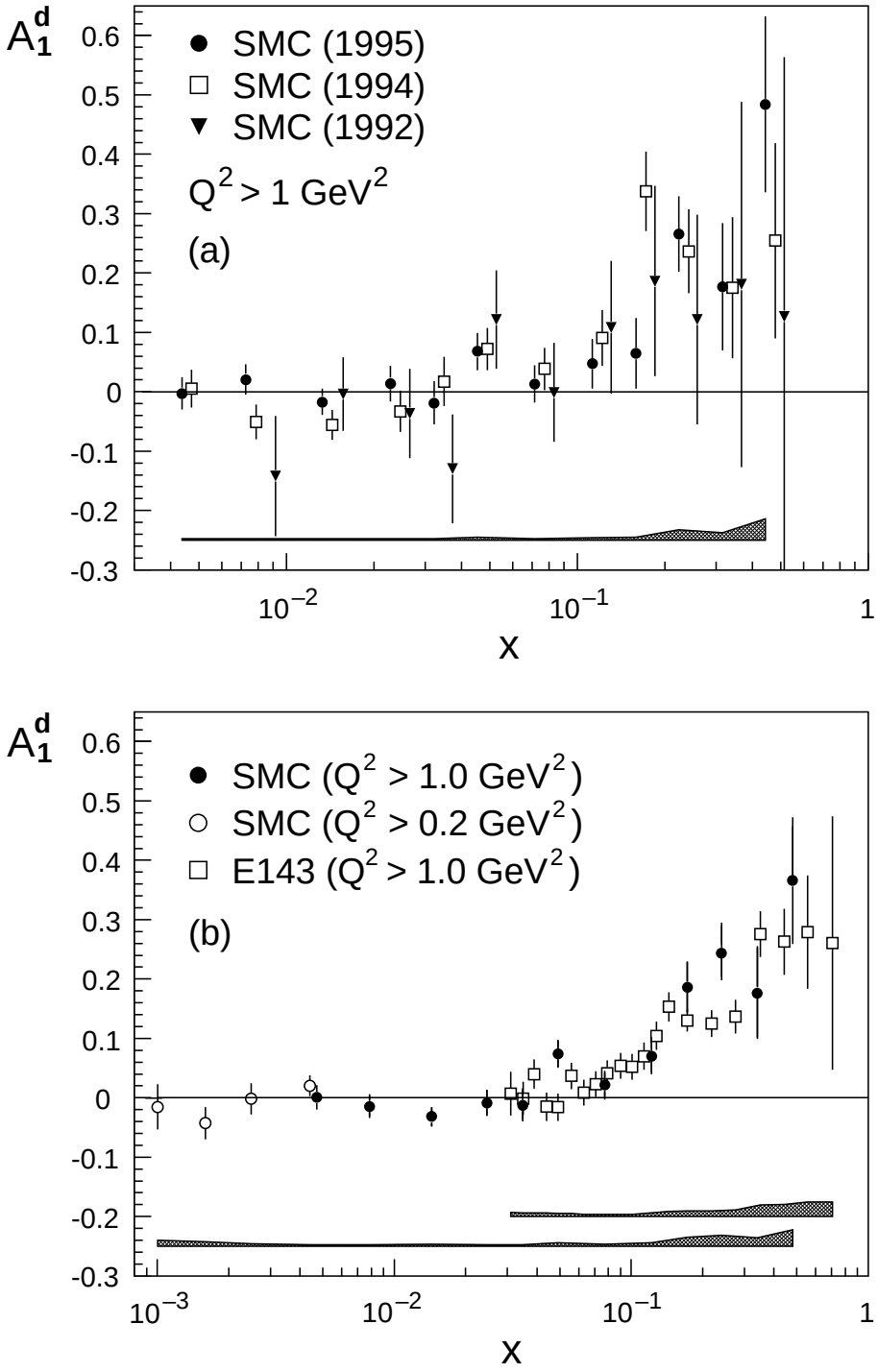

Figure 3: The virtual-photon deuteron asymmetry $A_1^{\rm d}$ as a function of the scaling variable x at the average Q^2 of each x bin. Only statistical errors are shown with the data points. In (a), results from the present measurement (1995) for $Q^2 > 1\,{\rm GeV}^2$ are compared to data taken previously with the same apparatus (1992 and 1994). The size of the systematic errors of the 1995 data is indicated by the shaded area; the systematic errors of the 1992 and 1994 data are of similar size. The combined 1992, 1994 and 1995 data are shown in (b); results from the SLAC E143 experiment [6] are shown for comparison.

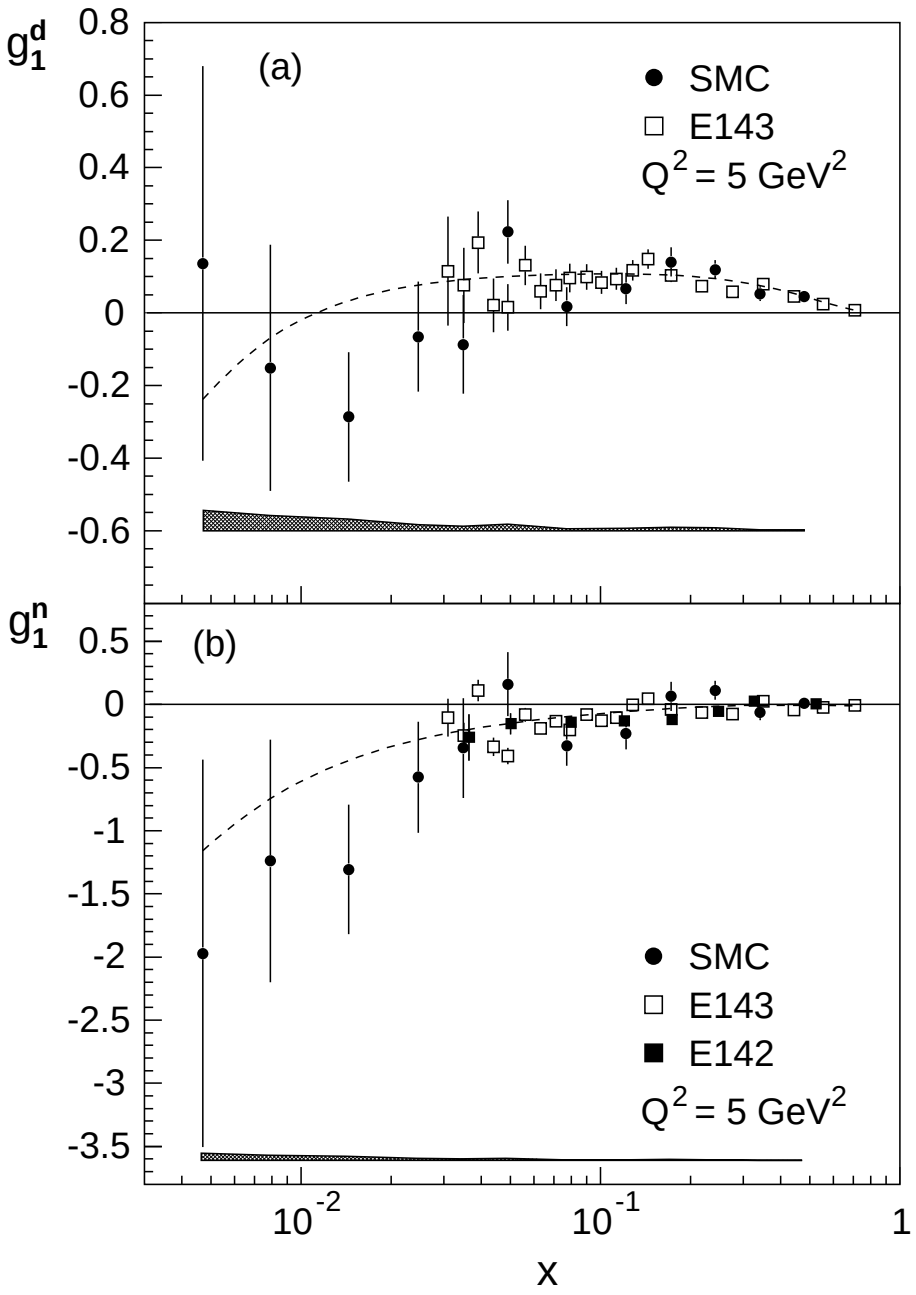

Figure 4: The spin-dependent structure functions $g_1^{\rm d}(x)$ (a) and $g_1^{\rm n}(x)$ (b), as a function of the scaling variable x evaluated at a common $Q_0^2 = 5$ GeV^2. Only statistical errors are shown on the data points; the size of the systematic errors is indicated by the shaded areas. Results from the SLAC E143 [6] and E142 [31] experiments are shown for comparison. The E142 data were evolved to $Q_0^2 = 5$ GeV^2 with the QCD fit discussed in the text; this fit is shown in (a) and (b) by the dashed line.